JOURNAL OF SOLID STATE CHEMISTRY 100, 229–245 (1992)

Vanadium Pentoxide and Vanadium Oxide Bronzes—Structural Chemistry of Single (S) and Double (D) Layer $M_xV_2O_5$ Phases

JEAN GALY*

Centre d'Elaboration de Matériaux et d'Etudes Structurales-Laboratoire d'Optique Electronique du CNRS, 29 Rue Jeanne Marvig, 31400 Toulouse, France

Received December 10, 1991; accepted March 16, 1992

DEDICATED TO STEN ANDERSSON

L'imagination est la reine du vrai
et le possible est une des provinces du vrai.
Charles Baudelaire

Investigation of the details of the V_2O_5 crystal structure shows the vanadium coordination to be purely square pyramidal SP, the single $[V_2O_5]$ layer S being built up by endless double strings of VO_5 SP associated by corner sharing. This unit allows to describe all the VOB's structures exhibiting S layers, i.e., α-$M_xV_2O_5$ (M = all elements), ε-, δ-, γ-$Li_xV_2O_5$, α'-$Na_xV_2O_5$, $Cu_{0.64}V_2O_5$. The structural mechanisms which govern the phase transitions $\varepsilon \rightarrow \delta$, $\delta \rightarrow \gamma$ have been described, as well as the transformations by crystallographic shears, slips, and VO_5 SP reversal of ε (or α) into the 3-D networks of β or β'-$M_xV_2O_5$ phases. The complete $Li_xV_2O_5$ system versus $f(T, x)$ is described and the evolution of the cell parameters for ε and γ phases is accounted for by introducing the puckering angle μ of the S layers. The demonstration of the slipping of the S layers quantified by shift Δ, expressed as a fraction or unit of the height of an octahedron, has made it possible to propose various original stackings for these layers; some ideal structures are described. A mechanism explaining the M intercalation between S layers shows that for large cations new layers are formed after shrinkage of two S layers giving double $[V_2O_5]$ layers D of the D4 and D4M types built up by endless quadruple strings and DZ type obtained from cross-linked double strings of VO_6 octahedra sharing edges and corners. This assumption is supported by the structure of the new VOB, τ-$Na_{0.70}V_2O_5$, which is an intergrowth of the D4 and DZ layer types. Using these units in combination with Δ slips has permitted a unifying description is given for all known structures: δ-$Ag_xV_2O_5$, δ-$Sr_xV_2O_5$, δ-$K_{0.5}V_2O_5$, ν-$Ca_{0.60}V_2O_5$, ν-$K_{0.62}V_2O_5$, ν-$Rb_{0.40}V_2O_5$, ν-$(NH_4)_{0.50}V_2O_5$, ε-$Cu_xV_2O_5$, ρ-$K_{0.50}V_2O_5$, . . . , and many other possibilities are suggested.

Introduction

Because of its wide applications, in pure form or via its numerous compounds, vanadium pentoxide has been the focus of much attention for many years. Structurally, the V_2O_5 network is viewed as exhibiting the characteristics of layer and crystallographic shear structure. Its formula yields a wide vanadium oxide bronze VOB family, $M_xV_2O_5$ (M = alkali, alkaline earth, metals), which shows several original $[V_2O_5]$ networks.

* Mailing address: CIEMES-LOE/CNRS, B.P. 4347, 31055 Toulouse Cedex, France.

0022-4596/92 $5.00

V_2O_5 and its derivatives have catalytic, physical, electrochemical properties directly related to their nonstoichiometric formulas and their atomic architectures.

The present discussion on crystal chemistry includes V_2O_5 and $M_xV_2O_5$ compounds characterized by single (S) and double (D) layer lattices.

This paper is organized as follows. In the first section we recall certain basic facts that must be present in any analysis. The V_2O_5 host lattice is a pure single layer S structure built up in one direction by infinite double strings of square pyramids SP VO_5 which share edges and corners along the short period of the layer (~ 3.7 Å) (Fig. 1) and held together by corner sharing in the remaining directions.

Following this discussion, it is shown that these VO_5 SP (Fig. 1) associated in double strings are the basis for discussion of S networks with particular emphasis on the $Li_xV_2O_5$ VOB, which is so important because of its properties.

Then it is shown how these S layers build double layers following M atoms intercalations in the V_2O_5 host lattice and the various adjustments in stacking layers versus the nature of M (M = Li, Na, K, Rb, Mg, Ca, Sr, Cu, Ag) (*1*).

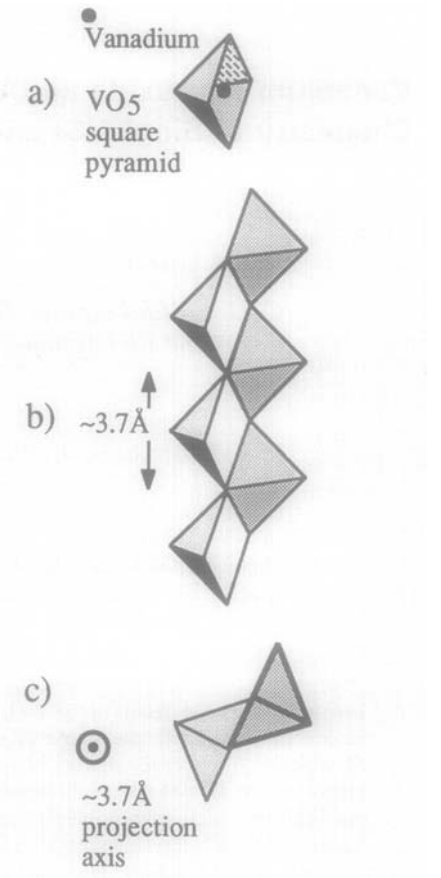

FIG. 1. Endless strings (b) of VO_5 square pyramids (a) sharing edges and corners; (c) ideal representation in projection along short 3.7 Å parameter.

Single Layer Structures

V_2O_5 Structure

The crystal structure was first investigated by Byström *et al.* (*2*), then by Bachmann *et al.* (*3*), and recently refined by Enjalbert and Galy (*4*). It has been inferred that the oxygen–vanadium coordination is fivefold (square pyramidal SP), but it has also been described as a distorted octahedra by taking into account a sixth oxygen, far from vanadium (2.791 Å). This long interatomic distance is opposite the shortest V–O bond directed toward the apex of the square pyramid. These choices entail widely different structures. First, chosing coordination number 5 for vanadium (CN5) leads to a V_2O_5 layer structure, while CN6 leads to a structure that can be considered similar to the R form of Nb_2O_5 (Fig. 2b) (Gruehn (5)). The latter structure is the result of the crystallographic shear operation $\frac{1}{2}$[100](100) occurring every two octahedra in the well known ReO_3-type network. This ambiguity has been with us for a long time. Our aim, in this paper is to resolve the issue.

The abnormal c parameter. Note first that the c parameter is wider than expected in V_2O_5 (4.368 Å) (Table I), i.e., ~3.830 Å (based on the diagonal of the SP along [100]

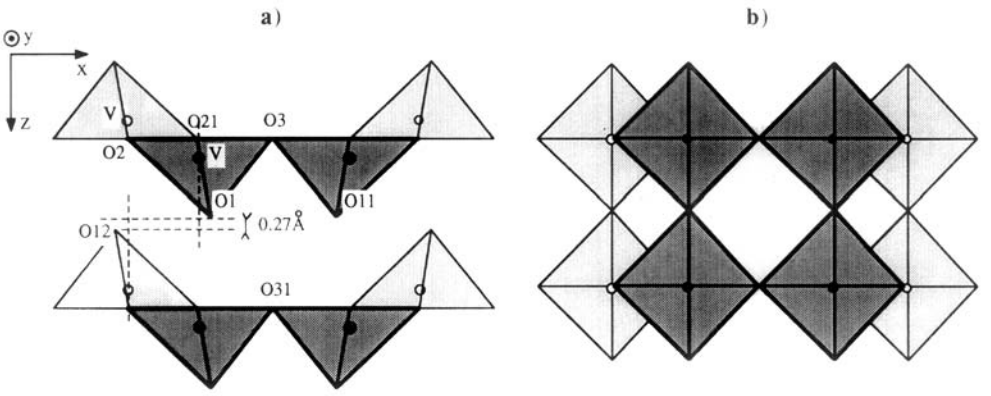

FIG. 2. Idealized V_2O_5 (a) and R-Nb_2O_5 (b) structures. Triangles represent square pyramids VO_5 (a) and squares NbO_6 octahedra (b). Thick lines and the darker shaded areas indicate a shift of $b/2$ compared with the thin lines and lighter shaded areas.

(11.512/3 Å)). A detailed analysis of the vanadium-oxygen bonding and its implication on oxygen–oxygen distances can account for this fact straightforward. To explain this (cf. Fig. 2a), note that the vanadium atom establishes a strong covalent bond (double bond character, vanadyl group V=O) with O1 at the apex of the SP (V–O1 = 1.577 Å) and is thereby pulled out of the basal plane by 0.470 Å; the opposite V–O12 interatomic distance is 2.791 Å, too long by far. This implies that there is no bonding. Hence the V_2O_5 layers cannot be held together via V–O12 interactions.

In addition, O–O repulsion occurs between oxygens O12 and O1 of adjacent layers, thus inducing a weak tilt of the V–O1 bond with respect to the [001] direction. The O1–O12 distance stabilizes at 3.003 Å, where a Van der Waals contact exists.

Another significant detail germane to our argument is the interspace of 0.27 Å between the planes parallel to (001) passing through O1 and O12 (cf. Fig. 2a).

These observations confirm that the long V–O12 interaction has been readily broken. Thus the V_2O_5 structure must be strictly described as $[V_2O_5]_n$ layers, built up from VO_5 square pyramids sharing edges and corners, the assembly being held together via Van der Waals interactions. These established basic facts will help us comprehend the structures of a range of V_2O_5 compounds.

$M_xV_2O_5$ vanadium oxide bronzes. These semi- or metallic conductors compounds possess extended homogeneous ranges of composition, that result from a nonstoichiometric intercalation of M cations within the $[V_2O_5]$ network. It may be assumed that the balance of the electric charges is due to the mixed valence of vanadium atoms (V^{5+}, V^{4+}). The $[V_2O_5]$ network for these compounds can be built up from:

—single layers of $[V_2O_5]$ type as in α-$M_xV_2O_5$ (M = almost all elements and x small (≤ 0.1)), α'-$Na_xV_2O_5$, γ-, ε-, and δ-$Li_xV_2O_5$;

—double layers of δ-$Ag_xV_2O_5$ type;

—a mixture of double and zig-zag layers, τ-$Na_{0.70}V_2O_5$ type;

—and, three dimensional (3-D) networks like the β-$Na_xV_2O_5$ and β'-$Li_xV_2O_5$ types.

The β-type structure, determined by Wadsley (*6*), as well as the β' form (Galy *et al.* (*7*)) exhibit tunnels parallel to [010],

TABLE I

CRYSTALLOGRAPHIC DATA OF SOME VANADIUM OXIDE BRONZES $M_xV_2O_5$

Compounds $M_xV_2O_5$	x	a(Å)	b(Å)	c(Å)	β(°)	V(Å^3)	Z	V/Z(Å^3)	Space group	References
V_2O_5		11.512(3)	3.564(3)	4.368(1)		179.2	2	89.6	*Pmmn*	(*4*)
Ideal V_2O_5		11.512	3.564	3.830		157.1	2	78.6	*Pmmn*	This paper
R-Nb_2O_5		12.79(1)	3.826(4)	3.983(3)	90.8(2)	194.9	2	97.5		(*5*)
α-$Li_xV_2O_5$	0.04	11.460(6)	3.554(2)	4.368(1)		177.9	2	88.9	*Pmmn*	(*9, 10*)
α-$Li_xV_2O_5$	0.10	11.495(5)	3.565(2)	4.386(8)		179.7	2	89.9	*Pmmn*	(*20*)
ε-$Li_xV_2O_5$	0.45	11.413(5)	3.563(2)	4.518(9)		183.7	2	91.8	*Pmmn* or $P2_1mn$	(*20*)
ε-$Li_xV_2O_5$	1.00	11.335(5)	3.589(3)	4.683(8)		190.5	2	95.3	*Pmmn* or $P2_1mn$	(*19*)
δ-$Li_xV_2O_5$	1.00	11.2423(8)	3.6018(3)	9.9054(9)		401.1	4	100.3	*Amma*	(*17*)
MgV_2O_5		11.019(5)	3.696(3)	9.965(5)		405.8	4	101.5	*Amma*	(*18*)
γ-$Li_xV_2O_5$	1.00	9.702(5)	3.607(2)	10.664(6)		373.2	4	93.3	*Pnma*	(*7*)
β-$Li_xV_2O_5$	0.30	15.464(6)	3.599(2)	10.068(6)	110.9(1)	523.3	6	87.2	*C2/m*	(*7*)
β'-$Li_xV_2O_5$		15.266(6)	3.618(2)	10.100(6)	107.7(1)	531.4	6	88.6	*C2/m*	(*7*)
α'-$Na_xV_2O_5$	1	11.318(5)	3.611(2)	4.797(3)		196.1	2	98.0	$P2_1mmn$	(*12*)
$Cu_xV_2O_5$	0.64	11.313	3.613	4.804		196.4	2	98.2	*Pmmn*	(*15*)
CaV_2O_5		11.347(3)	3.605(3)	4.892(3)		200.1	2	100.0	*Pmmn*	(*14*)
NaV_2O_4F		11.318(5)	3.609(2)	4.802(3)		196.1	2	98.1	*Pmmn*	(*13*)
τ-$Na_xV_2O_5$	0.70	11.648(2)	3.650(7)	8.879(1)	90.9(1)	377.4	4	94.4	*C2/m*	(*26*)
δ-$Ag_xV_2O_5$	0.68	11.742(8)	3.667(3)	8.738(5)	90.5(1)	376.2	4	94.1	*C2/m*	(*22*)
δ-$Sr_xV_2O_5$	0.50	11.759(8)	3.695(3)	8.789(5)	91.83(1)	381.9	4	95.5	*C2/m*	(*29*)
δ-$K_xV_2O_5$	0.50	11.68(1)	3.662(3)	9.48(1)	92.1(1)	405.2	4	101.3	*C2/m*	(*30*)
ν-$Ca_xV_2O_5$	0.60	11.805(2)	3.709(1)	9.270(2)	101.9(1)	396.2	4	99.0	*C2/m*	(*31*)
ν-$K_xV_2O_5$	0.62	11.63(1)	3.668(3)	9.55(1)	101.5(1)	399.2	4	99.8	*C2/m*	(*30*)
ν-$Rb_xV_2O_5$	0.40	11.63(4)	3.664(8)	9.75(3)	101.2(1)	407.6	4	101.9	*C2/m*	(*32*)
ν-$(NH_4)_xV_2O_5$	0.50	11.814(2)	3.674(2)	9.80(1)	102.7(1)	415.0	4	103.7	*C2/m*	(*33*)
ε-$Cu_xV_2O_5$	0.85	11.780(8)	3.691(3)	8.876(5)	111.8(1)	358.3	4	89.6	*C2/m*	(*34*)
ρ-$K_xV_2O_5$	0.50	11.607(3)	3.674(1)	18.670(8)		796.2	8	99.5	*Ccmm*	(*35*)

which are more or less filled by M cations. The nature of the various structural possibilities with variations in M has already been explained (Galy *et al.* (*8*)) and is not of paramount importance for a further discussion.

Basic Single Layer S Structures

α-$Li_xV_2O_5$ type. This structure established by Galy *et al.* (*9, 10*) is directly obtained from V_2O_5, a small amount of lithium (less than $x = 0.10$) being introduced between the layers on sites that can be described as trigonal prisms (Table I). The space group is identical to that of V_2O_5, i.e., *Pmmn*, with all vanadium crystallographic sites being identical and accommodating the small amount of V^{4+} cations (Fig. 3).

α'-$Na_xV_2O_5$ type. The α' phase exists for $0.70 \leq x \leq 1$ and is closely related to α-$Li_xV_2O_5$ (Table I), but with a major difference, though. The space group $P2_1mn$—*hkl* extinctions as for *Pmmn*— exhibits two different sites for vanadium atoms (*11, 12*). Electronic localization has been clearly revealed in the structure of α'-NaV_2O_5 ($x = 1$)

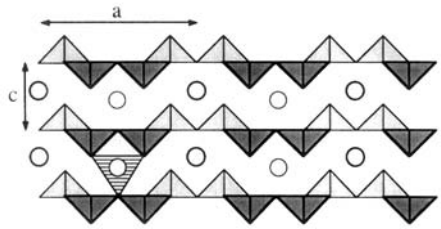

FIG. 3. Ideal representation of the α-phase. Triangles represent VO_5 square pyramids and circles M atoms. Thick lines and the darker shaded areas indicate that both triangles and circles are shifted by $b/2$ compared with thin ones.

the size of the two SP being typical for V^{5+} and V^{4+}. The confirmating demonstration was done by means of the synthesis and crystal structure determination of NaV_2O_4F (only V^{4+}) (Carpy and Galy (*13*)). This compound is strictly isostructural with α-$Li_xV_2O_5$ having the space group *Pmmn*, which has also been attributed to CaV_2O_5 (Bouloux and Galy (*14*). The $Cu_xV_2O_5$ structure ($x = 0.64$) determined by Christian *et al.* (*15*) is related to α-phases in spite of the high copper content.

γ-$Li_xV_2O_5$ type. Compound homogeneity range was found to be $0.88 \leq x \leq 1$ and the structure exhibits puckered $[V_2O_5]_n$ layers in which, for the first time, the electronic localization has been established (Table I). Thus two $[V^{5+}O_5]$ and $[V^{4+}O_5]$ square pyramids of widely different sizes where observed. The lithium between layers is octahedrally surrounded by oxygens (Galy *et al.*

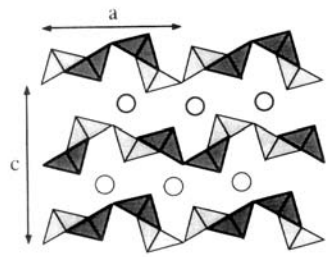

FIG. 4. Ideal representation of the γ-phase.

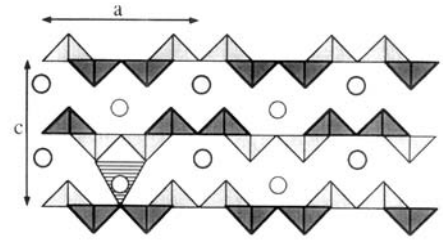

FIG. 5. Ideal representation of the δ-phase.

(*16, 7*)). Figure 4 schematically depicts an ideal structure of this phase.

δ-$Li_xV_2O_5$ type. This layered structure has been determined by Cava *et al.*'s (*17*). It consists of $[V_2O_5]_n$ layers of the V_2O_5 type, alternatively shifted by b/2 along [010] (Table I). This implies a doubling of the c parameter. Lithium atoms are surrounded tetrahedrally (Fig. 5) The assigned space group *Amma* implies equivalent vanadium sites in spite of the formal formula $LiV^{5+}V^{4+}O_5$. Again, MgV_2O_5, a hypovanadate (vanadate IV) earlier isolated by Bouloux *et al.* (*18*), is isostructural to δ-LiV_2O_5 (see Table I).

For the space groups, δ-LiV_2O_5 and MgV_2O_5, appear to behave as α'-NaV_2O_5 ($P2_1mn$) and the family V_2O_5, α-LiV_2O_5, CaV_2O_5, and NaV_2O_4F (*Pmmn*), suggesting that an electronic localization could occur, making the space group $A2_1ma$ more suitable for the δ phase; the centric space group corresponding exactly to MgV_2O_5.

M Intercalation between S Layers

Apart from the α phase, common to all $M_xV_2O_5$ oxide bronze families, only the smallest alkali or earth-alkali cations like Li, Na, Mg, and Ca seem to intercalate between S layers; there exists only a single phase for α'-Na and stoichiometric compounds for Ca and Mg. Lithium yields several structures as composition and temperature are varied. Our research effort must now form on a better understanding of how $Li_xV_2O_5$ phases evolves.

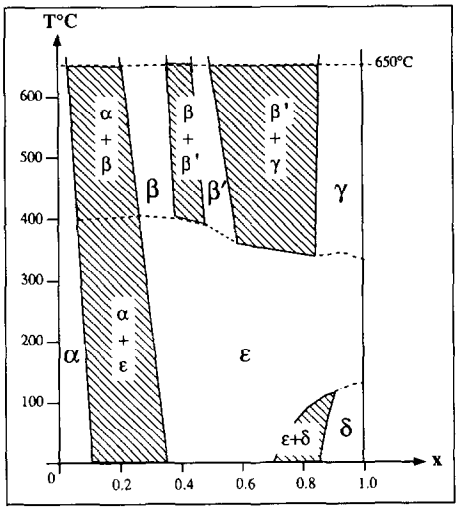

FIG. 6. Diagram $f(T, x)$ of the various homogeneity ranges of the α, β, β', and δ phases, according to data provided by Murphy (*19*) and Galy (*7*).

The lithium case—$Li_xV_2O_5$. After investigating this system by solid-state chemistry, at around 650°C (Galy *et al.* (*7*)), soft chemistry was used to introduce lithium atoms into the V_2O_5 network. This led to a range of new phases as shown by Murphy *et al.* (*19*) and (Dickens *et al.* (*20*)). The results are summarized below:

Room temperature (*19, 20*)		$0 < x \leq 0.10$	α
		$0.35 \leq x \leq 0.70$	ε
		$0.90 \leq x \leq 1$	δ
150°C	(*19*)	$0 < x \leq 0.10$	α
		$0.35 \leq x \leq 1$	ε
650°C	(*7*)	$0 < x \leq 0.04$	α
		$0.22 \leq x \leq 0.37$	β
		$0.44 \leq x \leq 0.49$	β'
		$0.88 \leq x \leq 1$	γ

From there a revised $f(T, x)$ diagram given in Fig. 6 can be inferred.

$Li_xV_2O_5$: $x(x < 1)$ and Temperature-Dependent Structural Evolution

Room Temperature

α-$Li_xV_2O_5$. The V_2O_5 structure favors the intercalation of Li, via the (100) face and mainly via the (010) face where large rhombic channels running parallel to [010] exist, thus producing this α-form so often adopted by several M cations for small values of x. This inturn leads to a decrease in cell parameter a, while b and c remain virtually constant (*19*).

ε-$Li_xV_2O_5$. The coexistence of phases of α- and ε- means that ε has a different structure, like α'-NaV_2O_5; i.e., the amount of V^{4+} increases as x augments. The cell exhibits important variation with x (*19, 20*), a decreasing and c increasing, while b does not vary significantly (see Table I). The increase in c is readily explained by the increasing number of lithium atoms between the layers. The a variation is not easy to understand but can be accounted for, by noting that Li, in its trigonal prism and firmly attached to four oxygens on one layer, attracts the apex oxygens, thus closing the angle between the SP sharing corners (Fig. 7). Incidentally note that the S layer is puckered, maximum puckering occuring when the puckering angle of the basal oxygen plane of SP, μ, is raised at an angle of 60° between SP. μ varies ideally from 0° for V_2O_5 up to 30°, allowing calculation of $a_{\text{pmin.}}$, the minimum value for parameter a of a $[V_2O_5]$ layer. Thus

$$a_{\text{pmin.}} = a_{V_2O_5} \cos(\mu/2) \quad \text{for } \mu = 30° \Rightarrow$$
$$a_{\text{pmin.}} = 11.12 \text{ Å}.$$

With respect to an accurate structure, i.e., taking into account the data provided

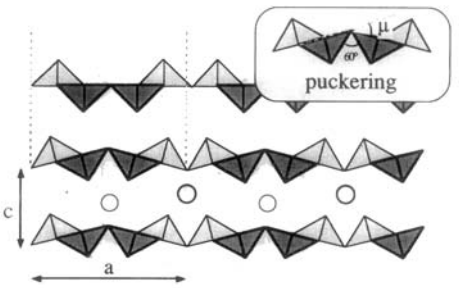

FIG. 7. Puckering of $[V_2O_5]$ layers.

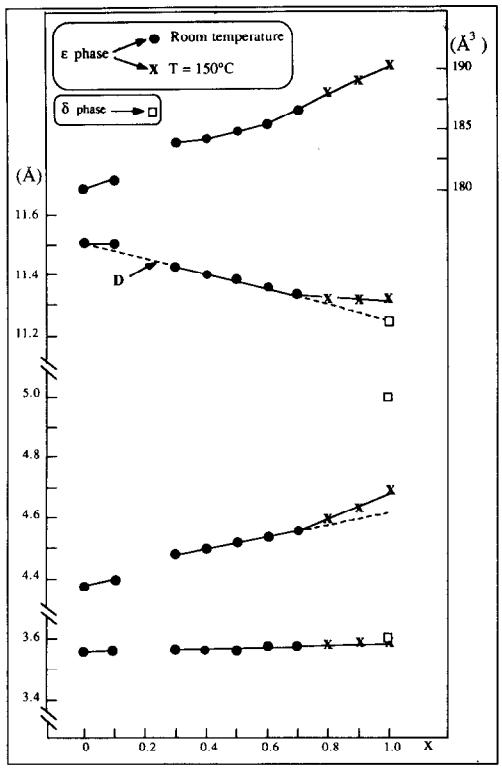

FIG. 8. Evolution of a, b, and c of the ε-phase versus x after (*19*).

by Enjalbert and Galy (*4*) for V_2O_5 (O1–O3 = 2.652 Å and O1–O12 = 3.003 Å), the O1–O11 closest contact should be similar to that of O1–O12. The smallest O1O3O11 angle calculated is 69°. This gives a puckering angle of 21° and hence a shortest a_ε of 11.32 Å. If we use the plot of Murphy *et al.* (*19*) of a_ε versus x, it evolves as a straight line, which extrapolated passes through $a_{V_2O_5}$. Then it is possible to derive a simple equation roughly representing the a_ε variation at room temperature (line D) (Fig. 8)

$$a_\varepsilon = -0.264\,x + 11.512$$

(for $x = 1$, if ε-phase existed, the a_ε value would have been approx. 11.248 Å).

δ-LixV$_2$O$_5$. As x still increases, a δ variety is formed and can be accounted for if one recalls that Li atoms filling up the trigonal channels along [010] grapple onto more and more O1 and O2 and drag along the $[V_2O_5]$ layers as they move over a distance $b/2$. Now, the movement of these layers places a concommitant demand for more space; as a result and correlatively c is observed to expand. Following this $[V_2O_5]$ layers rearrangement, which brings about the formation of the δ network, two sites are available for lithium that is one in an SP form (O31O1O1O11O11) and another as a tetrahedron, T (O31O31O1O11) (see Fig. 9). The latter is chosen by Li (Fig. 9) as shown by Cava *et al.* (*17*).

When magnesium is substituted for lithium in this structure, the a parameter is smaller, corresponding to maximum puckering of the $[V_2O_5]$ layers (*18*); a circumstance reasonably attributed to the double charge of Mg that makes it more polarizing than Li.

T = 150°C

—The α-phase still exists but the ε-phase now covers the whole range for $0.35 \leq x \leq 1$ after the occurrence of the phase transition that transforms δ into ε (*16*).

—Thermal energy allows the $[V_2O_5]$ layers of δ to be rearranged and to produce the

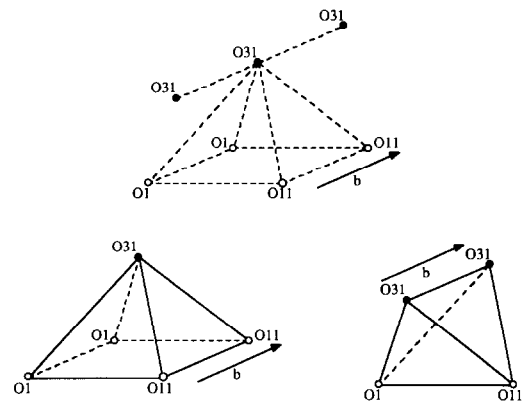

FIG. 9. Possible SP and T sites for Li in δ-LiV_2O_5.

more efficient packing encountered in ε ($V_\delta/2$ = 200 Å^3, $V_{\varepsilon,150°C}$ = 190 Å^3). The rearrangement is accompanied by an abrupt decrease of c following the Li "jump" into the largest voids of the trigonal prisms; concommitantly, following the $\delta \Rightarrow \varepsilon$ transition, the puckering slightly recedes and a increases.

The evolution of a_ε and c_ε for $0.7 < x \leq 1$ is linear and slightly above the extrapolated lines obtained at room temperature (Fig. 8). This is because the results are obtained at a higher temperature. The value of a_ε for x = 1 derived from the curve, i.e., ~ 11.33 Å, is in good agreement with the value calculated above and corresponds to maximum puckering, i.e., ~ 11.320 Å, confirming the assumption that this ubiquitous structural feature is linked to the maximum chemical composition ε-$Li_xV_2O_5$ under these experimental conditions.

T = 650°C

Here the α phase has the smallest homogeneity range and the ε phase for increasing x values has been transformed into three phases, β, β', and γ, separated by biphasic domains (*7*).

This structural phase transition α (or ε) $\Rightarrow$ β can be accounted for by a mechanism that is based on the aforementioned arguments (β' exhibits a similar $[V_2O_5]$ network).

In Fig. 10A, idealized views of α or ε (Fig. a) and β (Fig. b) are given; in phase β the ideal upper limit corresponds to x = 0.33 (*6*). Note that this limit is close to the minimum of the phase ε. The upper limit for β' is x = 0.66 (*7*).

If a crystallographic shear (CS) is applied in the plane $(\bar{1}01)$ of ε-LiV_2O_5 with a periodicity of $3/2a$, $3/2[100](\bar{1}01)$, the structure is alternately sliced into slabs of types 1 and 2 (Fig. 10B).

Then, the S layers in these slabs are ended by an oxygen vacancy (square in Fig. 10C). In each slab, the S layers slip by Δ (along the straight arrow) and stack, dragging a rearrangement of oxygens in square pyramids (indicated by curved arrows) and forming puckered double layers of types 1 and 2 which can be held together at the level of oxygen vacancies by filling them. The VO_5 SP reversal follows the classical scheme (Fig. 11). The alternate repetition of layers 1 and 2 build the $[V_2O_5]$ network of the β phase with its typical channels developed along [010]. Similarly the β' phase can be derived, the inserted Li atoms occupying different positions in the channel.

The formation of the γ phase can also be explained as follows.

LiV_2O_5: Structural Evolution versus Temperature

For the highest Li concentration allowed by these synthesis techiques (*19, 20, 16*), i.e., x = 1, three phases, δ, ε, and γ, are found across the entire temperature range from room temperature up to 650°C.

The structural rearrangement of the $[V_2O_5]$ network which occurs at approx. 120°C following the phase transition $\delta \Rightarrow \varepsilon$ has already been described.

The problem, is now to account for the mechanism which transforms ε into the γ phase around 350°C. Thermal perturbation allows the structure to improve S layer packing (V_γ = 174.5 Å^3 against V_ε, 150°C = 190 Å^3). a_γ is drastically diminished. Thus from Table I: a_γ = 9.702 Å while the evaluated a_ε = 11.320 Å; the a_γ value being dramatically below the idealized, a_χ ~ 11.248 Å, that corresponds to the largest observed puckering angle μ = 30°. Thus the layers must be even more puckered. To this, blocks of two SP, as indicated in Fig. 12a, "rotate," giving an S layer analogous to that observed when Mo substitutes for V in the monoclinic $V_{2-x}Mo_xO_5$ phases ($0.23 \leq x \leq 0.30$) (Fig. 12b) (Kihlborg (*21*)). Layers alternately slip along the indicated vector. The S organization allows a new important puckering to take place, one SP being able to complete the coordination sphere of V

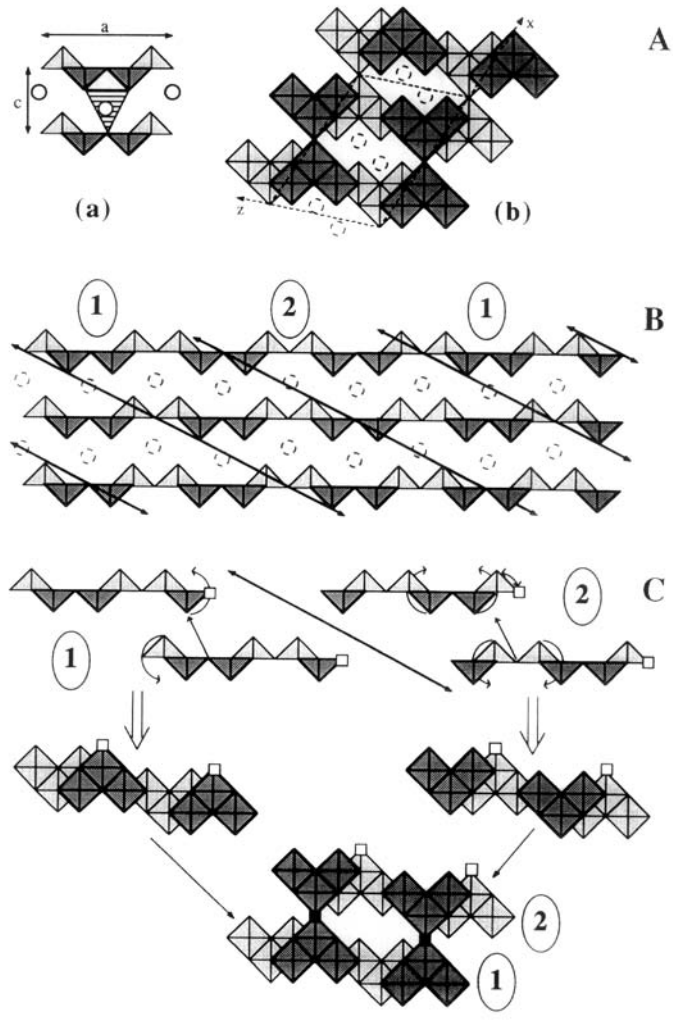

FIG. 10. Phase transition $\varepsilon \Rightarrow \beta$ (or β'). (A) Schematic views of the projection along [010] of (a) α (or ε)-$Li_xV_2O_5$; (b) β (or β')-$Li_xV_2O_5$. (B) Slicing of the α (or ε)-$Li_xV_2O_5$ by the crystallographic shear 3/2[100](101) giving alternate 1 and 2 slabs. (C) Reconstruction of the 3-D network of β-$Li_xV_2O_5$ after: SP reorganization into slabs; their association in double layers 1 and 2 after the Δ slip; and their final association by corner sharing.

up to six. At the limit the VO_6 octahedron shares an edge with a VO_5 SP. The corresponding maximum puckering angle $\mu_{max.}$ is 90°, giving $a_{ypmin.} = 8.140$ Å (Fig. 12c). In fact puckering in the phase γ is not so dramatic since the observed μ, $\mu \sim 65°$, is limited by the presence of lithium atoms between the layers (Fig. 12d).

This type of endless strings formed by the blocks of two SP extending along [010] and sharing corners to form the puckered $[V_2O_5]$ layers parallel to (001) are also found in potassium titanate $K_2Ti_2O_5$ studied by Andersson and Wadsley (22). In this structure, the unfolding of $[Ti_2O_5]_n^{2n-}$ layers (puckering angle is close to zero) permits accommoda-

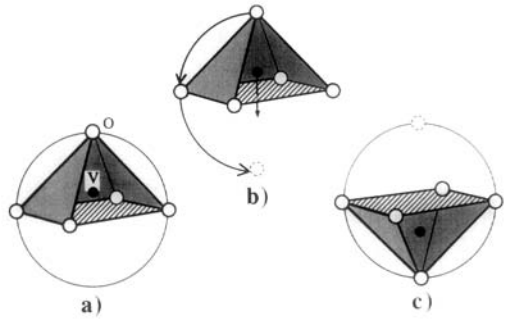

FIG. 11. Reversal of the square pyramid VO_5.

tion of more intercalated cations, i.e., two potassiums ($K_2Ti_2O_5$: monoclinic, $C2/m$, $a = 11.37$ Å, $b = 3.80$ Å, $c = 6.62$ Å, $\beta = 100.1°$, $Z = 2$).

With respect to γ-$Li_xV_2O_5$, it is easy to imagine intermediate structures by progressively unfolding the $[V_2O_5]$ layer, the puckering angle μ tending toward zero and x being able to reach two. The extra Li ion intercalation producing these structures illustrate the principle of the chemical twinning on the unit cell level developed by Andersson and Hyde (*23*).

Under conditions of solid state reactions (at 650°C) the γ-$Li_xV_2O_5$ phase no longer exist for $x > 1$; a disproportion of V^{4+} into V^{5+} and V^{3+} has been proved. However, this intercalation permitting phase γ to be extended up to $Li_2V_2O_5$ might be performed by "soft" chemistry. $Li_2V_2O_5$ in any case will be the ultimate composition obtained for γ-like structure (all vanadiums are tretravalent), since V^{3+} cannot be accommodated in the SP of such layers, its coordination being strictly octahedral.

Comments—Prospects

All phases of the $Li_xV_2O_5$ system ($0 \leq x \leq 1$) have been described and their transformation, versus composition and/or temperature, explained simply in terms of reorganization of the VO_5 SP, CS and slips. The known $M_xV_2O_5$ structures made up of single layer S, with M = α-, ε-, δ-Li, α'-Na, Ca or Mg, and NaV_2O_4F, are directly related. Even the β- and β'- high-temperature 3-D structures have been correlated to their mother structure ε-$Li_xV_2O_5$ prepared at room temperature.

During phase transformation, the ability of $[V_2O_5]_n$ layers to slip has been noted, as exemplified by $\varepsilon \Rightarrow \delta$ and $\delta \Rightarrow \varepsilon$ transitions.

This easily rearrangement enables us to propose a few other structural possibilities (that could readily be enlarged in the same spirit) that open up new prospects in the field of S-$M_xV_2O_5$ phases insofar as the interpretation of certain unknown, badly crystallized structures is concerned, thus allowing new chemical syntheses. By varying the ex-

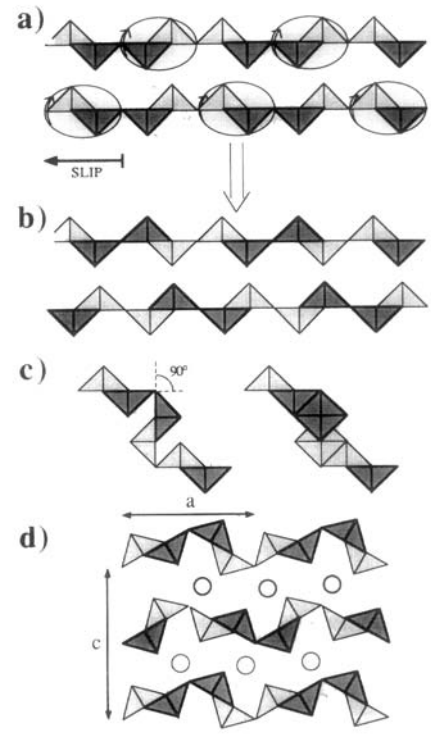

FIG. 12. Proposal for the structural mechanism transforming ε into γ. (a) Reorganization of SP; (b) S layers of $V_{2-x}Mo_xO_5$ type; (c) maximum possible puckering $\mu_{max.} = 90°$; (d) γ-LiV_2O_5 phase.

perimental conditions or modifying the mixtures of small M elements, or by partially replacing the vanadium element by other transition element, as already reported by Galy *et al.* (*24*) for the first mixed vanadium oxide bronzes $M_xV_{2-y}T_yO_5$ (M = Li, Na; T = Mo, W), or fluorine to oxygen, alternative illustrated by the first vanadium oxide fluoride bronzes, $Na_xV_2O_{5-y}F_y$ (*25*), new compounds could be synthesized.

Rules

The $[V_2O_5]_n$ layers remain parallel and are allowed to slip along [010] by $b/2$ steps and along [100] by simple steps quantified by Δ. The chosen unit Δ, based on the diagonal of the VO_5 SP, approx. 3.8 Å, is also the height Oc of an octahedron. Thus Δ is expressed in terms of a fraction or unit of Oc.

Proposals based on the α-$Li_xV_2O_5$ Layer Sequence

$\Delta \Rightarrow 1/2\ Oc$. If all the layers slip in sequence, a monoclinic cell is obtained, the M atoms being inserted in the octahedral or large square pyramid sites thus created (Fig. 13A).

$\Delta \Rightarrow 1\ Oc$. Then two alternatives arise; either: (1) the layers move as in the preceding analysis (Fig. 13B(a)) and yield a monoclinic cell with the M atoms having two possible crystallographic sites, that is, in the large square channels built up by bicapped trigonal prisms sharing faces along b, or in a rhombic channel defined by monocapped trigonal prisms sharing triangular faces along b; (2) the layers are alternately moved. Sites, similar to the former ones (those described in Fig. 13B(a)) can accommodate M atoms (Fig. 13B(b)). The cell is orthorhombic with c doubling.

$\Delta \Rightarrow 3/2\ Oc$. Layers slip alternately by $\Delta \Rightarrow 1/2\ Oc$. The resulting cell is orthorhombic and c is doubled. M atoms are inserted into two types of large channels, built up along b, by large tricapped trigonal prisms sharing faces or trigonal prisms which share rectangular faces (Fig. 13C).

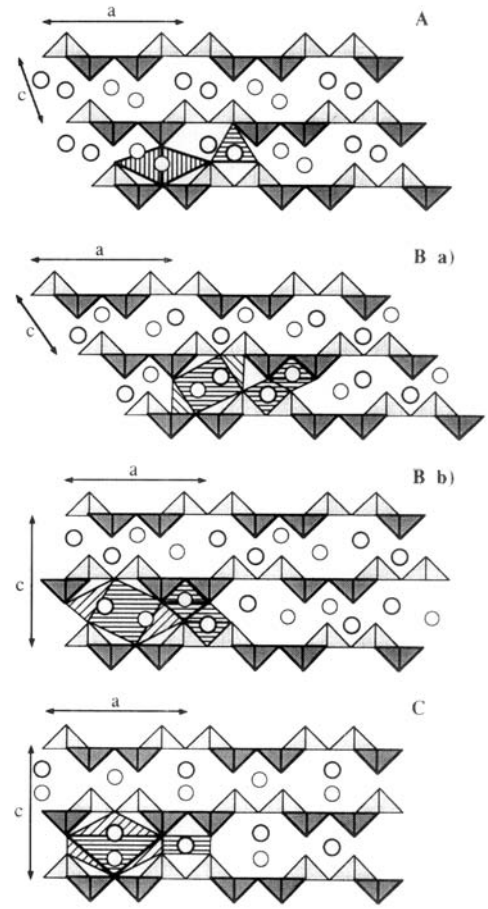

FIG. 13. Proposal of some $[V_2O_5]$-like S layer packings for $M_xV_2O_5$ phases: (A) $\Delta = 1/2Oc$ sequential slip; (B) (a) $\Delta = 1Oc$ sequential slip; (b) $\Delta = 10c$ alternate slip; (C) $\Delta = 3/2Oc$.

Proposal Based on the δ-$Li_xV_2O_5$ Layer Sequence

An example is given in Fig. 14 and corresponds to a slip $\Delta \Rightarrow 1\ Oc$. The orthorhombic cell is maintained but drastic changes allow for a possible insertion of M: thus (1) a large channel containing octahedral sites; these large octahedra share two opposite edges develop as a chain along [010]; (2) another

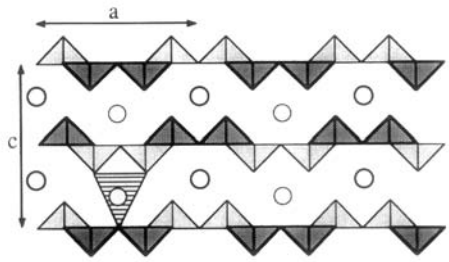

FIG. 14. Proposal for a possible packing of δ-$[V_2O_5]$-like S layer with $\Delta = 1\ Oc$.

channel, built up by two rhombic prisms associated through their bases along *b*.

Remark. The crystallographic sites indicated in the various figures, as areas of possible *M* intercalation, limit the *x* value to 2. For monovalent *M* cations *x* can be equal to or less than 2 and for divalent $x < 1$; in both cases the upper limit corresponds to $[V_2O_5]$ layers containing only tetravalent vanadiums. Thus any proposal for introducing V^{3+} (strict CN6) in these layers is pure nonsense.

From Single (S) to Double Layer (D) Structures

Intercalation Mechanism and Formation of D Layers

As already been noted vanadium oxide bronzes exhibiting S layers are formed for low charge–low size cations, i.e., Li and Na with exceptions for Mg and Ca which form definite MV_2O_5 compounds.

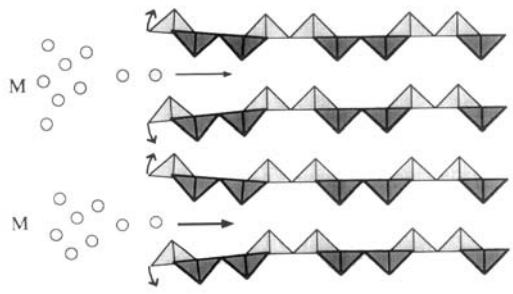

FIG. 15. *M* atoms entering V_2O_5 network.

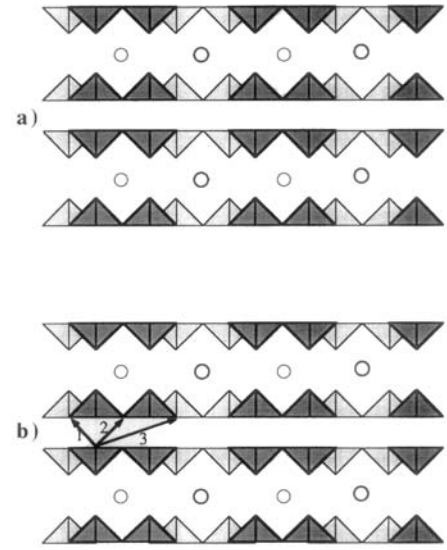

FIG. 16. (a) Reversal of VO_5 SP. (b) Possible slips (1, 2, and 3) for transforming VO_5 SP into VO_6 octahedra.

What takes place when *M* increases in size and charge?

Figure 15 illustrates our proposal. For these *M* atoms, insertion and diffusion occur more easily every two layers because of distortions at the edge of the lattice created by their entry. Subsequently some VO_5 SP turn backward following the classical scheme (Fig. 11) and the layers slip as vanadium rearranges in the empty space and bond with oxygens (Figs. 16a,b).

Three types of slip can occur that give rise to:

1 ⇒ D4 layer (Fig. 17a);
2 ⇒ D4M layer, mirror image of the former (Fig. 17b);
3 ⇒ DZ layer (Fig. 17c).

From the known structures, it is clear that in these double layers vanadium atoms depicted as occupying octahedra are in fact displaced in the upper part of the octahedra close to the *M* layer (or attracted, to form

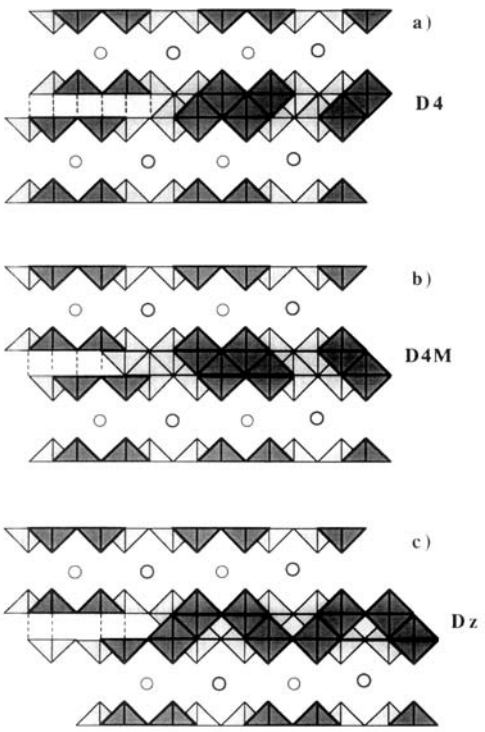

FIG. 17. Formation of D4, D4M, and DZ layers.

the V = O bond). The median plane of the double layers D exhibits weak V–O bonds, generally V–O ≈ 2.2 to 2.3 Å.

The Key Structure: τ-$Na_{0.70}V_2O_5$

Recently a new τ-$Na_{0.70}V_2O_5$ VOB has been prepared and its structure determined by Savariault *et al.* (*26*). It is a monoclinic compound, *C2/m*, a = 11.648(2) Å, b = 3.650(7) Å, c = 8.879(1) Å, β = 90.93(2)°, Z = 4.

During structure refinement one vanadium atom and three oxygens fully occupied their crystallographic sites. The other independent vanadium and two oxygens belonging to its coordination sphere were located in two neighboring sites, each with 50% occupancy. The resulting structure is a perfect intergrowth of two phases (A and B) with the same cell parameters but different V double layers (D4 for A and DZ for B), and the sodium atoms lying between them (Fig. 18). The intergrowth plane results from a D4 layer type followed by another of the DZ type. In the interlayer space AB, note that the sites for Na atoms (i.e., rhombic + trigonal prisms) are mirror images of those existing between two homologous layers AA. The Na sites between BB layers are different (trigonal prisms + octahedra).

The existence of this new phase strengthens the model for the double layer formation proposed above.

Double Layer Structures (D)

All structures can be described with the same underlying basis of $[V_2O_5]_n$ layers, which are more or less displaced along [100] by quantified Δ slips that generate classical regular polyhedra between the layers for inserted cations.

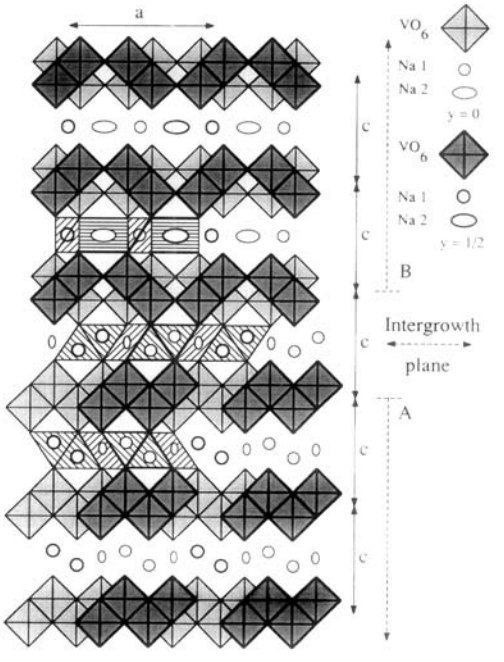

FIG. 18. Idealized structure of the τ-$Na_{0.70}V_2O_5$ phase; intergrowth of two types of crystals A and B.

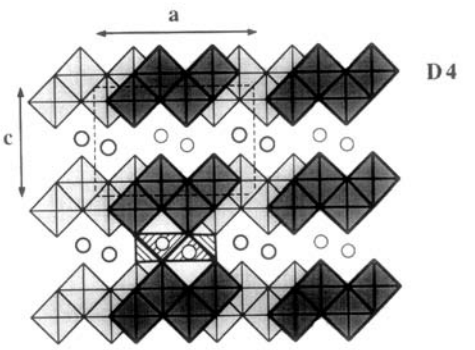

FIG. 19. Ideal drawing of the δ-$Ag_xV_2O_5$ VOB (D4) structure corresponding to $\Delta = 0$ *Oc*.

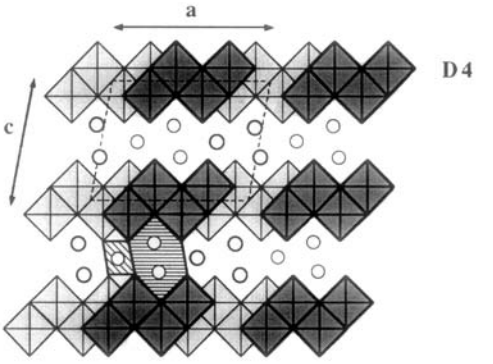

FIG. 20. Ideal drawing of VOB structures D4 with $\Delta = -1/2$ *Oc*.

First Prototype: δ-$Ag_xV_2O_5$ ($\Delta = 0$ Oc)

This first D-VOB was synthesized and its structure determined by S. Andersson (*27*). It exhibits the typical D4 type layers with vanadium atoms in distorted octahedra (CN = 5 + 1). The silver atoms between the layers are described as fivefold coordinated to oxygens; the description of Ag polyhedra can be extended and depicted as a monocapped trigonal prism.

As reported by Andersson these double layers are similar to those of titanium oxide bronze Na_xTiO_2 (Andersson and Wadsley (*28*)).

It is noteworthy that the $[V_2O_5]_n$ layers are packed without relevant slipping ($\beta \sim 90°$) and according to the rules put forward in a preceding paragraph, $\Delta = 0$ *Oc*.

This structure is also adopted by the VOB phase δ-$Sr_xV_2O_5$ (*29*) and δ-$K_xV_2O_5$ ($x \sim 0.50$) (*30*).

An ideal drawing is given in Fig. 19. The inserted atoms are accommodated in monocapped trigonal prisms which share a rectangular face, making a chain parallel to [010].

VOB D4 Structure with $\Delta = -1/2$ Oc

The ideal structure obtained after displacement $\Delta = -1/2$ *Oc* and illustrated in Fig. 20 fits in well with the structure of $Ca_xV_2O_5$ VOB with $x = 0.60$, which is the first model of the ν phases. In this context, calcium atoms partially occupy crystallographic sites which are quasi-aligned in a plane parallel to (001) (*31*). This model also corresponds to the ν-$M_xV_2O_5$ phases with M = K with $x \sim 0.62$ (*30*), Rb with $x \sim 0.40$, or again NH_4 with $x \sim 0.50$ (*33*).

VOB D4 Structure with $\Delta = +1$ Oc

Figure 21 shows the resulting ideal monoclinic structure after a displacement $\Delta = +1$ *Oc*. The built up network resides between the layers, trigonal pyramides (threefold axis along [100]) sharing rectangular faces and developing large rectangular tunnels running along [010] and octahedral sites

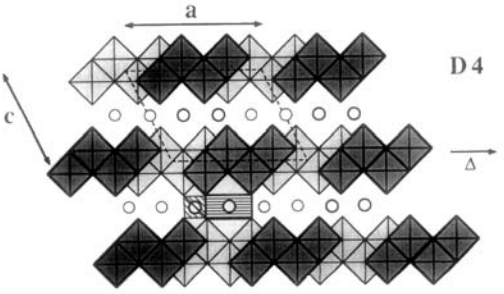

FIG. 21. Ideal drawing of the VOB structures D4 with $\Delta = 1$ *Oc*.

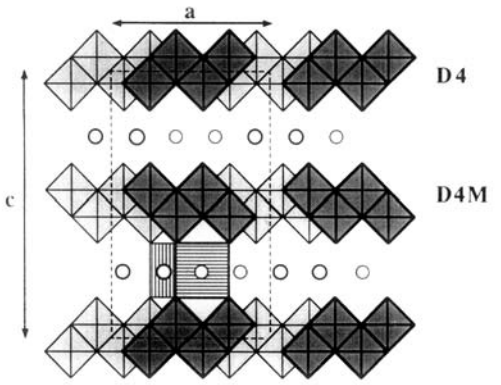

FIG. 22. Schematic drawing of $K_xV_2O_5$ VOB with $x \approx 0.50$ exhibiting alternate packing of D4 and D4M layer types.

sharing edges and generating a chain along [010].

Such an arrangement of $[V_2O_5]_n$ layers corresponds to the ε-$Cu_xV_2O_5$ ($x = 0.85$) studied by Galy *et al.* (*34*). In reality copper atoms partly occupy two different sites, a somewhat different situation from those indicated on the idealized figure.

VOB D4 and D4M Structures

By interlaying D4 and D4M and using various slips Δ several original structures can be created.

Only the structure of ρ-$K_xV_2O_5$, VOB with $x \sim 0.5$ just determined by Savariault *et al.*, is indicated in Fig. 22; it is formed by alternate stacking of D4 and D4M layers without Δ displacement sandwiching K atoms (*35*). Potassium atoms partially occupy sites at the centre of a cube which share faces along *Oy* and trigonal prisms associated by rectangular faces along [010].

VOB DZ Structures

Similar variations are also possible using DZ-type layers.

While pure phase has not been prepared the B crystal of the τ-$Na_{0.70}V_2O_5$ intergrowth VOB illustrates a first example (*26*). Nevertheless, we are confident that these phases, the ideal structure of which is illustrated in Fig. 23, will soon be synthesized.

Conclusion

On the basis of a deep understanding of the V_2O_5 structure establishing the strict oxygen pyramidal coordination of vanadium, the structural unit, an endless double string of SP sharing edges and corners with the ~3.7-Å period (Fig. 24a), allows to describe all the structures of the S layers of the $M_xV_2O_5$ phases and make structural relationships or phase transition mechanisms easier to explain and to depict.

Then this should enable us to put forward new proposals involving various packings of S layers sandwiching *M* intercalated cations.

The S-layer shrinkage, with the extension of the vanadium coordination from fivefold up to sixfold gives rise to the formation of double layers D4 (or D4M) characterized by quadruple strings of octahedral sharing edges along [010] (~3.7 Å period) (Fig. 24b) or again DZ layers built up by cross-linked double strings of octahedra (Fig. 24c).

The rule set forth for the relative layer displacement, Δ, expressed as a fraction or a unit of the height *Oc* of an octahedron, has been successfully applied to the classification of various classes.

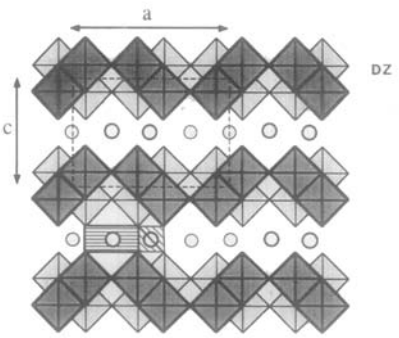

FIG. 23. Ideal structure built up by DZ layer type.

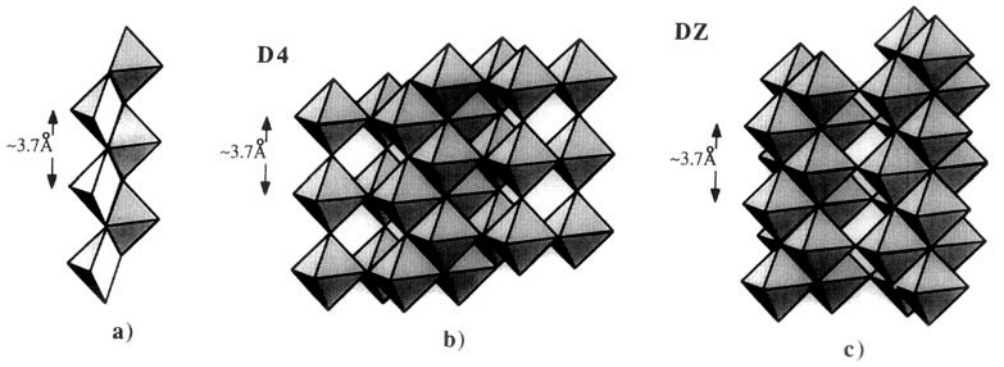

FIG. 24. Various endless strings encountered: (a) double string of VO_5 square pyramid in S layers; (b) quadruple string of VO_6 octahedra in D4 and D4M layers; (c) cross-linked double string of VO_6 octahedra in DZ layers.

These results suggest further precize structural investigations so as to follow or predict the S- or D-layer packing versus the nature, stoichiometry, charge, and size of intercalated cations.

The versatility of all these $M_xV_2O_5$ phases, the so-called vanadium oxide bronzes, containing vanadium in both 5^+ and 4^+ states located in square pyramids of oxygens (CN5 can be extended to trigonal bypyramid) or octahedra, accommodating a variation of the ratio V^{5+}/V^{4+} following the stoichiometry in intercalated cation M defined by parameter x is one of the most remarkable family in the field of solid state chemistry.

Acknowledgments

The author thanks CNRS and NFR for making his stay at the Universities of Stockholm and Lund in Sweden during which this paper was written.

I am also grateful to Professor Barry Ninham (Canberra) for his fruitful comments.

References

1. J. GALY, *Mater. Res. Soc. Symp. Proc.* **156,** 25 (1989).
2. A. BYSTRÖM, K. A. WILHELMI, AND O. BROTZEN, *Acta Chem. Scand.* **4,** 1119 (1950).
3. H. G. BACHMAN, F. R. AHMED, AND W. H. BARNES, *Z. Kristallogr.* **115,** 110 (1961).
4. R. ENJALBERT AND J. GALY, *Acta Crystallogr., Sect. C* **42,** 1467 (1986).
5. R. GRUEHN, *J. Less-Common Met.* **11,** 119 (1966).
6. A. D. WADSLEY, *Acta Crystallogr.* **8,** 695 (1955).
7. J. GALY, J. DARRIET, AND P. HAGENMULLER, *Rev. Chim. Miner.* **8,** 509 (1971).
8. J. GALY, J. DARRIET, A. CASALOT, AND J. B. GOODENOUGH, *J. Solid State Chem.* **1,** 339 (1970).
9. J. GALY, Thèses, Bordeaux, 1965 and 1966.
10. A. HARDY, J. GALY, A. CASALOT, AND M. POUCHARD, *Bull. Soc. Chim. Fr.* **4,** 1056 (1965).
11. J. GALY, A. CASALOT, M. POUCHARD ET P. HAGENMULLER, *C. R. Acad. Sci.* **262,** 1055 (1966).
12. A. CARPY AND J. GALY, *Acta Crystallogr., Sect. B* **31,** 1481 (1985).
13. A. CARPY AND J. GALY, *Bull. Soc. Fr. Miner. Cristallogr.* **94,** 24 (1971).
14. J. C. BOULOUX AND J. GALY, *J. Solid State Chem.* **16,** 385 (1976).
15. P. A. CHRISTIAN AND H. MÜLLER-BUSCHBAUM, *Z. Naturforsch.* **298,** 713 (1974).
16. J. GALY AND A. HARDY, *Acta Crystallogr.* **19,** 432 (1965).
17. R. J. CAVA, A. SANTORO, D. W. MURPHY, S. M. ZAHURAK, R. M. FLEMING, P. MARSH, AND R. S. ROTH, *J. Solid State Chem.* **65,** 63 (1986).
18. J. C. BOULOUX, I. MILOSEVIC, AND J. GALY, *J. Solid State Chem.* **16,** 393 (1976).
19. D. W. MURPHY, P. A. CHRISTIAN, F. J. DISALVO, AND J. V. WASZCZAK, *Inorg. Chem.* **18,** (10), 2800 (1979).
20. P. G. DICKENS, S. J. FRENCH, A. T. HIGHT, AND M. F. PYE, *Mater. Res. Bull.* **14,** 1295 (1979).
21. L. KIHLBORG, *Acta Chem. Scand.* **21,** 2495 (1967).
22. S. ANDERSSON AND A. D. WADSLEY, *Acta Chem. Scand.* **15,** 663 (1961).

23. S. ANDERSSON AND B. G. HYDE, *J. Solid State Chem.* **9,** 92 (1974).
24. J. GALY, J. DARRIET, AND D. CANALS, *C. R. Acad. Sci.* **264,** 579 (1967).
25. J. GALY AND A. CARPY, *C. R. Acad. Sci.* **268,** 2195 (1969).
26. J. M. SAVARIAULT, J. L. PARIZE, AND J. GALY, *Solid State Comm.*, in press.
27. S. ANDERSSON, *Acta Chem. Scand.* **19,** 1371 (1965).
28. S. ANDERSSON AND A. D. WADSLEY, *Acta Crystallogr.* **15,** 201 (1962).
29. J. C. BOULOUX, J. GALY, AND P. HAGENMULLER, *Rev. Chim. Miner.* **T11,** 48 (1974).
30. M. POUCHARD AND P. HAGENMULLER, *Mater. Res. Bull.* **2,** 799 (1967).
31. A. KUTOGLU, *Z. Kristallogr.* **162,** 263 (1983).
32. P. STROBEL, *J. Solid State Chem.* **66,** 95 (1987).
33. R. BENCHIFRA, Thèse, Université du Maine, 1990.
34. J. GALY, D. LAVAUD, A. CASALOT, AND P. HAGENMULLER, *J. Solid State Chem.* **2,** 531 (1970).
35. J. M. SAVARIAULT AND J. GALY, *J. Solid State Chem.*